Biophysical Chemistry, 37 (1990) 171–181
Elsevier

BIOCHE 01475

Oxygen binding to partially oxidized hemoglobin

Analysis in terms of an allosteric model

Lorenzo Cordone, Antonio Cupane, Maurizio Leone, Valeria Militello and Eugenio Vitrano

Istituto di Fisica dell' Università and GNSM-CISM, 90123 Palermo, Italy

Received 18 January 1990
Revised manuscript received 22 February 1990
Accepted 22 February 1990

Hemoglobin, partially oxidized; Oxygen uptake; Allosteric equilibrium; Allosteric model; Methemoglobin

We report on oxygen binding to partially oxidized (aquomet) hemoglobin. The fractional saturation with oxygen is evaluated by deconvoluting the optical absorption spectra, in the 500–700 nm wavelength region, in terms of oxyhemoglobin, deoxyhemoglobin and methemoglobin spectral components. Experiments have been performed with auto-oxidized samples and with samples obtained by mixing ferrous hemoglobin with fully oxidized hemoglobin (mixed samples). An increase in oxygen affinity and a decrease in cooperativity are observed on increasing the amount of ferric hemoglobin in the sample. A high cooperativity ($n_H \approx 2$) is maintained even in the presence of 50–60% ferric hemes. Moreover, for equal amounts of methemoglobin the oxygen affinity is lower and the cooperativity higher for mixed samples than for those auto-oxidized. The results are analyzed within the framework of a modified Monod-Wyman-Changeux allosteric model taking into account the effects brought about by the presence of oxidized hemes and of $\alpha\beta$ dimers. The distribution of ferric subunits within the tetramers in fully deoxygenated and fully oxygenated samples, as derived from the model, provides details on the cooperative behavior of partially oxidized hemoglobin.

1. Introduction

The effect of partial auto-oxidation on the oxygen binding reaction of hemoglobin as well as the validity of the allosteric models proposed as mechanistic interpretations of hemoglobin functional properties are two issues of general interest in this field. In the case of methemoglobin, the allosteric equilibrium is less displaced towards the R conformation than for oxyhemoglobin [1,2], as a consequence of the slightly different position of the iron atom with respect to the porphyrin plane [3,4]. One, therefore, expects that the presence of a fraction of oxidized hemes sizably affects the overall behavior of the protein during oxygenation. For this reason we have undertaken a study aimed at obtaining data on oxygen binding to partially oxidized hemoglobin. The data are rationalized in terms of a modified Monod-Wyman-Changeux (MWC) [5] model.

Correspondence address: L. Cordone, Istituto di Fisica dell' Università and GNSM-CISM, 90123 Palermo, Italy.

2. Materials and methods

2.1. Samples

Hemoglobin was prepared from the blood of healthy donors, following a standard procedure [6]. Hemoglobin preparation was begun immediately after drawing the blood. The concentrated (approx. 15%, w/v) oxyhemoglobin

0301-4622/90/$03.50 © 1990 Elsevier Science Publishers B.V. (Biomedical Division)

stock solution was fractionated in 1-ml aliquots stored in liquid nitrogen. The amount of methemoglobin in each concentrated oxyhemoglobin fraction was assessed by measuring the absorbance at 630 nm prior to use and was found to be less than 1% in every case. Concentrated methemoglobin stock solutions were prepared as described by Perutz [7].

All measurements reported in this work were performed at $T = 25\,^{\circ}C$ under experimental conditions of 6×10^{-5} M heme, 0.1 M phosphate buffer (pH 7.0).

2.2. Reference spectra

Reference spectra of oxyhemoglobin (HbO_2), methemoglobin (Hb^{3+}) and deoxyhemoglobin (Hb) were obtained as follows. An HbO_2 sample, prepared by dilution of a concentrated aliquot immediately after melting, was used to obtain the HbO_2 reference spectrum. The sample was then oxidized by adding 1 mg of potassium ferricyanide directly into the cuvette and then the Hb^{3+} reference spectrum was recorded. The same sample was then reduced by the direct addition of approx. 2 mg of sodium dithionite into the cuvette, followed by measuring the Hb reference spectrum.

Spectrophotometric measurements, within the wavelength range 700–500 nm, were performed on a Cary 118C ultraviolet/visible spectrophotometer controlled by a PC-IBM. All of the spectra were digitized with 0.5-nm steps. Statistical analysis was performed off-line with an HP-1000 A 900 computer.

2.3. Oxygen uptake in auto-oxidized samples

A 100 ml sample of HbO_2 was allowed to auto-oxidize at $T = 25\,^{\circ}C$. Aliquots (5 ml each) were withdrawn at various time intervals and used to measure the oxygen equilibrium curve at the particular methemoglobin concentration reached. Oxygen equilibrium curves were determined using a tonometric method [6]. Measurements of an oxygen equilibrium curve typically took about 4 h. At each oxygen partial pressure, the entire spectrum from 700 to 500 nm was measured. The spectra were analyzed as a linear combination of the previously measured reference spectra according to the following equation:

$$A_i = \left(f_{HbO_2} A_i^{HbO_2}\right) + \left(f_{Hb} A_i^{Hb}\right) + \left(f_{Hb^{3+}} A_i^{Hb^{3+}}\right) + B \qquad (1)$$

where A_i is the absorbance of the sample at wavelength λ_i; $A_i^{HbO_2}$, A_i^{Hb} and $A_i^{Hb^{3+}}$ denote the absorbance, at the same wavelength λ_i, of the reference spectra of HbO_2, Hb and Hb^{3+}, respectively; f_{HbO_2}, f_{Hb} and $f_{Hb^{3+}}$ represent the respective fractions of HbO_2, Hb and Hb^{3+} present in the sample. The constant B was added in order to take into account eventual baseline shifts. The conservation relationship is expressed as:

$$f_{HbO_2} + f_{Hb} + f_{Hb^{3+}} = K \qquad (2)$$

where K is the ratio of the protein concentration in the actual sample to that used to measure the reference spectra. This quantity was floated in the curve fitting to account for possible differences in concentration between the actual and reference samples. The values of K were found to be in the range 1 ± 0.02 for all measurements.

The four independent parameters f_{HbO_2}, f_{Hb}, $f_{Hb^{3+}}$ and B were found by minimizing the quantity:

$$\Gamma^2 = \sum_i \left[A_i(\text{observed}) - A_i(\text{calculated})\right]^2 / \left[N - P\right] \qquad (3)$$

where N is the number of data points (≈ 400) and P the number of optimizing parameters. A typical example is shown in fig. 1. Fig. 1 also shows the difference between the measured and calculated spectra. It should be noted that the most relevant contribution to the difference spectrum arises from small shifts in the monochromator of the Cary 118C spectrophotometer (of the order of ± 0.2 nm) in agreement with the findings of Philo et al. [8]. The standard deviations of the parameter values were all found to be less than ± 0.002. During the measurement of each oxygen equilibrium curve, the fraction of oxidized protein, $f_{Hb^{3+}}$, was found to remain almost constant, the largest increase in $f_{Hb^{3+}}$ being below 0.02 in every case.

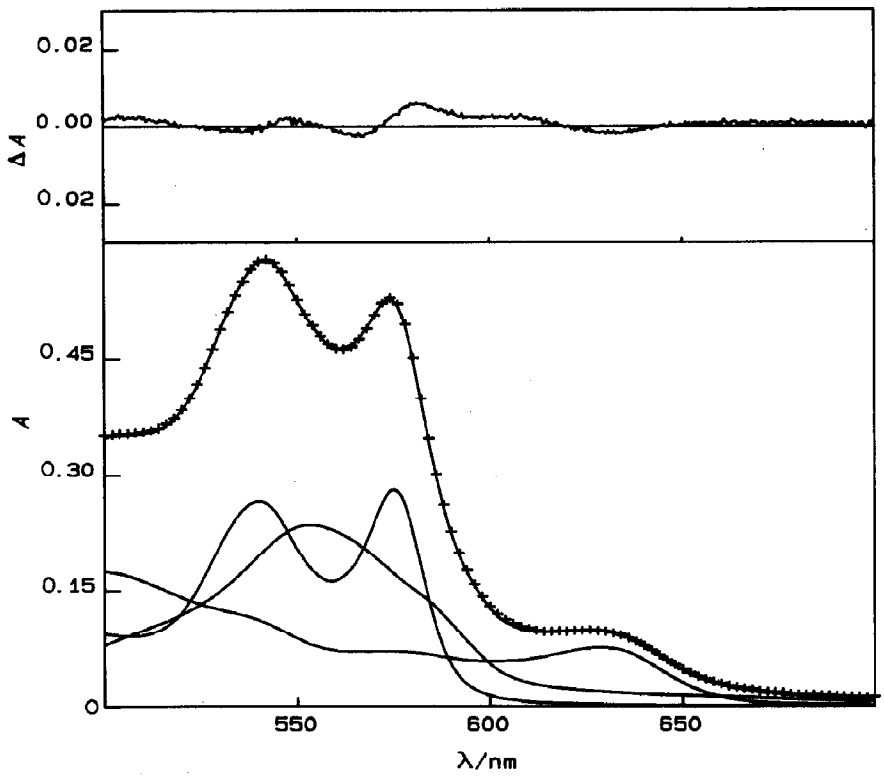

Fig. 1. (Bottom panel) Deconvolution of a typical experimental spectrum as a linear combination of the reference spectra of HbO_2, Hb and Hb^{3+}. (+) Experimental points; (———) reference spectra (multiplied by the suitable fractions) and the synthesized profile. For the sake of clarity not all of the experimental points are reported. For this example, $f_{HbO_2} = 0.331$, $f_{Hb} = 0.323$, $f_{Hb^{3+}} = 0.346$ and $B = 0.008$. (Top panel) Difference between experimental and synthesized spectrum. $\Delta A(\lambda)$ is defined as $\Delta A(\lambda) = A_{observed}(\lambda) - A_{calculated}(\lambda)$.

2.4. Oxygen uptake in 'mixed samples'

These measurements were performed by determining the oxygen equilibrium curves for samples obtained by mixing immediately before measurements suitable fractions of 100% Hb^{3+} and nominally 100% HbO_2 solutions. The same procedure as described above was used for carrying out measurements and analyses.

2.5. Auto-oxidation kinetics

The auto-oxidation kinetics of an HbO_2 sample was followed by a spectrophotometric method. In view of the rather long times involved, particular care was taken to work under sterile conditions in order to avoid bacterial contamination. Spectra were recorded automatically at selected time intervals and analyzed as described above to yield the fractions of Hb, HbO_2 and Hb^{3+} as a function of time. The fraction of deoxyhemoglobin was found to be less than 0.01. The total protein concentration remained almost constant throughout the measurements, although a slight decrease (less than 0.02, probably due to protein denaturation) was observed after lengthy intervals.

3. Results

Fig. 2 shows the Hill plots relative to some typical oxygen equilibrium curves in the presence of various fractions of oxidized hemoglobin (data refer to auto-oxidized samples). In agreement with

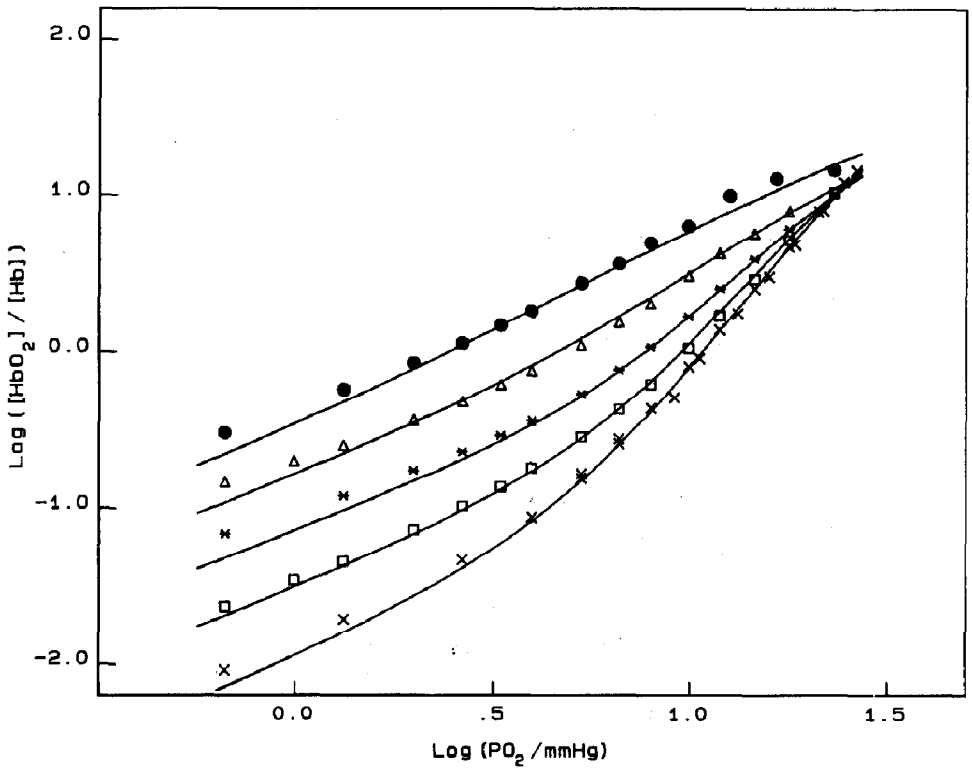

Fig. 2. Hill plots relative to some typical oxygen equilibrium curves obtained in the presence of various amounts of oxidized hemoglobin (auto-oxidized samples). (×) $f_{Hb^{3+}} = 0.005$, (□) $f_{Hb^{3+}} = 0.187$, (*) $f_{Hb^{3+}} = 0.385$, (△) $f_{Hb^{3+}} = 0.64$, (●) $f_{Hb^{3+}} = 0.84$. (———) Best fits obtained using the model described in the text and the set of parameters reported in table 1.

previously published data [9], both the logarithm of oxygen pressure at half hemoglobin saturation (log P_{50}) and the slopes of the experimental curves at $P_{O_2} = P_{50}$ (Hill coefficient, n_H) decrease with increasing fraction of Hb^{3+}. Although the data shown in fig. 2 are clearly insufficient to determine the asymptotes of the Hill plots, it is evident that the effect of increasing amounts of Hb^{3+} is large at the lower end of the curves (low oxygen pressure and hemoglobin saturation) and tends to vanish at the upper end (high oxygen pressure and hemoglobin saturation). This behavior confirms the hypothesis that the presence of increasing amounts of oxidized subunits alters the equilibrium constant K_T (in the terminology of the MWC model), but leaves the equilibrium constant K_R unchanged.

The dependence of log P_{50} and n_H upon the fraction of Hb^{3+} is demonstrated in fig. 3. An interesting feature of the data in fig. 3 is that samples with equal Hb^{3+} fractions exhibit higher log P_{50} values in 'mixed', than in auto-oxidized samples. The same effect, although less pronounced, is also observed for the n_H values. Interestingly, n_H values of approx. 2 are maintained up to Hb^{3+} fractions of approx. 0.5–0.6, despite the presence of Hb^{3+} causing a decrease in cooperativity.

Mansouri and Winterhalter [10] have reported the existence of α-β heterogeneity in the kinetics of auto-oxidation. In order to determine the ratio α^{3+}/β^{3+} in our auto-oxidized samples, we performed measurements of HbO_2 auto-oxidation kinetics as shown in fig. 4, in which the continuous line is a best fit of the experimental points with a single exponential. The results shown in fig. 4 do not provide evidence in support of the existence of α-β heterogeneity in our samples during

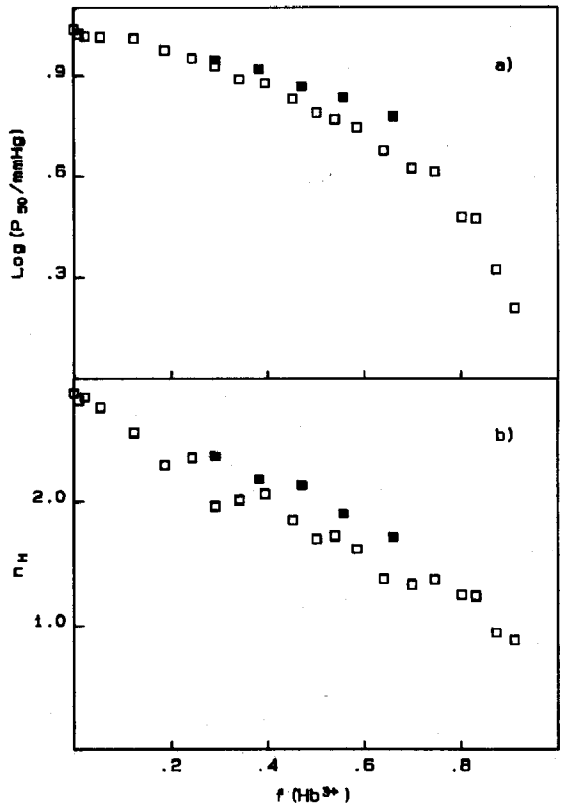

Fig. 3. Log P_{50} (a) and n_H (b) as a function of the fraction of oxidized hemoglobin. (□) Auto-oxidized samples; (■) mixed samples.

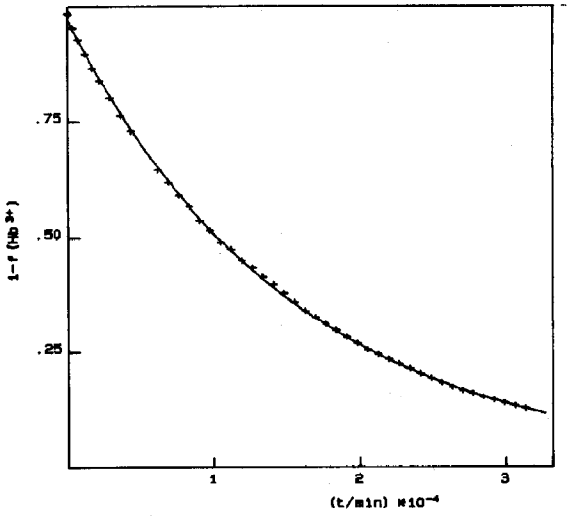

Fig. 4. Kinetics of auto-oxidation of HbO_2. (+) Experimental points; (———) best fit with a single exponential.

HbO_2 auto-oxidation. The difference we observed on comparison with the data reported by Mansouri and Winterhalter may be due to the different experimental conditions (6×10^{-5} M in heme protein concentration, 0.1 M phosphate buffer (pH 7.0) and $T = 25\,^{\circ}C$ in the present work; 5×10^{-4} M in heme protein concentration, 0.1 M phosphate buffer (pH 7.2) and $T = 37\,^{\circ}C$ in ref. 10). On the basis of the results shown in fig. 4, we shall therefore assume that all samples contain equal amounts of α and β ferric subunits.

4. The model

The results obtained in this study can be rationalized within the framework of an allosteric model which takes into account the presence of $\alpha\beta$ dimers and ferric subunits.

4.1. Auto-oxidized samples

4.1.1. Definition of symbols used and assumptions

T_i^k and R_i^k (i, $k = 0$–4; $i + k \leq 4$) indicate the hemoglobin tetramers in the T and R states, respectively, with i oxygen molecules bound and k ferric subunits. D_i^k (i, $k = 0$–2; $i + k \leq 2$) refers to the hemoglobin dimer with i oxygen molecules bound and k ferric subunits. Hemoglobin dimers are assumed to be in the R state. $L = T_0^0/R_0^0$ is the usual MWC allosteric parameter while K_R and K_T are the intrinsic oxygen dissociation constants of ferrous hemoglobin (i.e., hemoglobin without ferric subunits) in the R and T states, respectively. $c_0 = (K_R/K_T)_0$, as usual.

M denotes the association constant for association of dimers to form tetramers in the R state. This association constant is assumed to depend only upon the quaternary conformation and not upon the number of oxygen molecules bound or the presence of ferric subunits.

The allosteric equilibrium for tetramers lacking ferric subunits is governed by the well-known relationship:

$$T_i^0/R_i^0 = L(c_0)^i \quad (i = 0\text{–}4)$$

The allosteric equilibrium for tetramers with k ferric subunits but lacking bound oxygen molecules is governed by

$$T_0^k/R_0^k = L(d)^k \quad (k = 0\text{–}4).$$

The parameter d is expected to be less than unity (the presence of a ferric subunit shifts the quaternary equilibrium towards the R state) but larger than c_0 (although methemoglobin is in the R state [11,12], its allosteric equilibrium is more shifted towards the T state than that of oxyhemoglobin [12]).

In order to describe the equilibria of tetramers with i oxygen molecules bound and k ferric subunits, we introduce the parameters

$$c_k = (K_R/K_T)_k \quad (k = 0\text{–}3)$$

as the ratio of the intrinsic oxygen dissociation constants of hemoglobin tetramers with k ferric subunits in the R and T states. We expect c_k to increase with increasing k. Indeed, the data in fig. 2 suggest that the presence of ferric subunits decreases K_T and leaves K_R unchanged. From the definitions above, it follows that:

$$T_i^k/R_i^k = L(d)^k (c_k)^i \quad (i, k = 0\text{–}4;\ i + k \le 4) \tag{4}$$

The oxygenation equilibria of the various species present in solution are expressed using eq. 4 and the following equations:

$$R_i^k = \binom{4-k}{i} (x)^i R_0^k;\ i, k = 0\text{–}4;\ i + k \le 4 \tag{5}$$

$$D_i^k = \binom{2-k}{i} (x)^i D_0^k;\ i, k = 0\text{–}2;\ i + k \le 2 \tag{6}$$

where $x = P_{O_2}/K_R$, and $\binom{4-k}{i} = (4-k)!/(4-k-i)!i!$ and $\binom{2-k}{i} = (2-k)!/(2-k-i)!i!$ are statistical factors.

The dimer $\leftrightarrow$ tetramer equilibria are expressed by:

$$R_0^0 = M(D_0^0)^2 \tag{7}$$

$$R_0^1 = 2M(D_0^0)(D_0^1) \tag{8}$$

$$R_0^2 = 6M(D_0^0)(D_0^2) = (3/2)M(D_0^1)^2 \tag{9}$$

$$R_0^3 = 2M(D_0^1)(D_0^2) \tag{10}$$

$$R_0^4 = M(D_0^2)^2 \tag{11}$$

From eq. 9 it follows that

$$(D_0^1)^2 = 4(D_0^0)(D_0^2) \tag{12}$$

It should be noted that in deriving eqs 5–12 we have neglected the effect of α-β inequivalence on both oxygenation and auto-oxidation of hemoglobin.

A comment concerning the derivation of eqs 9 and 12 is appropriate. It is known that the splitting of one hemoglobin tetramer into dimers does not occur statistically but along the $\alpha_1 - \beta_2$ interface [13]. By considering a tetramer as composed of two equivalent $\alpha\beta$ dimers, the entire R_0^2 population can be divided into two classes: $(R_0^2)_I$, i.e., tetramers in which the two ferric subunits are in the same dimer and $(R_0^2)_{II}$, i.e., tetramers in which the two ferric subunits are in different dimers. The dimer-tetramer equilibria are expressed by:

$$(R_0^2)_I = 2M(D_0^0)(D_0^2)$$

$$(R_0^2)_{II} = M(D_0^1)^2$$

By considering that in auto-oxidized samples $(R_0^2)_I = R_0^2/3$ and $(R_0^2)_{II} = 2R_0^2/3$, eqs 9 and 12 follow. Eq. 12 could have been obtained in a more direct way by considering that, for auto-oxidized samples, ferric subunits are statistically distributed within $\alpha\beta$ dimers. However, we preferred to use the argument reported above, since it can be straightforwardly extended to the case in which the distribution of ferric subunits within dimers is not statistical, as for mixed samples.

4.1.2. Saturation function

The saturation function is defined as:

$$Y = \left[\sum_{i,k} i(R_i^k + T_i^k) + \sum_{i,k} iD_i^k\right]/C_0 \tag{13}$$

where C_0 is the total hemoglobin concentration expressed in heme. The summation relative to tetramers spans from 0 to 4 (with $i + k \le 4$), while that relative to dimers spans from 0 to 2 (with $i + k \le 2$).

Using eqs 4–12, it is possible to express the saturation function in the form:

$$\begin{aligned} C_0 Y = {} & A_1(D_0^0)^2 + A_2(D_0^0)^{3/2}(D_0^2)^{1/2} \\ & + A_3(D_0^0)(D_0^2) + A_4(D_0^0)^{1/2}(D_0^2)^{3/2} \\ & + A_5(D_0^0) + A_6(D_0^0)^{1/2}(D_0^2)^{1/2} \end{aligned} \tag{14}$$

where

$$A_1 = 4Mx\{[1+Lc_0]+3x[1+L(c_0)^2]+3x^2[1+L(c_0)^3]+x^3[1+L(c_0)^4]\}$$

$$A_2 = 12Mx\{[1+Lc_1d]+2x[1+L(c_1)^2d]+x^2[1+L(c_1)^3d]\}$$

$$A_3 = 12Mx\{[1+Lc_2(d)^2]+x[1+L(c_2)^2(d)^2]\}$$

$$A_4 = 4Mx\{1+Lc_3(d)^3\}$$

$$A_5 = 2x\{1+x\}$$

$$A_6 = 2x$$

From eq. 14 we see that Y is a function of seven adjustable parameters: L, c_k $(k=0\text{–}3)$, d and K_R. The dimer ↔ tetramer association constant M is fixed at the value 4×10^5 M^{-1} at 25°C [14,15]. The two unknown quantities in eq. 14, i.e., (D_0^0) and (D_0^2), are found by means of the closure relationships below.

4.1.3. Closure relationships

The first relationship expresses the fact that the sum of the concentrations of all species present must be equal to the total hemoglobin concentration, i.e.,

$$4\sum_{i,k=0}^{4}(R_i^k+T_i^k)+2\sum_{i,k=0}^{2}D_i^k=C_0 \qquad (15)$$

where C_0 is the heme concentration and summations are restricted to the usual conditions ($i+k\le4$ for tetramers and $i+k\le2$ for dimers).

Using eqs 4–12 one has:

$$C_0 = B_1(D_0^0)^2+B_2(D_0^0)^{3/2}(D_0^2)^{1/2}+B_3(D_0^0)(D_0^2)+B_4(D_0^0)^{1/2}(D_0^2)^{3/2}+B_5(D_0^2)^2+B_6(D_0^0)+B_7(D_0^0)^{1/2}(D_0^2)^{1/2}+2(D_0^2) \qquad (16)$$

where

$$B_1 = 4M\{[1+L]+4x[1+Lc_0]+6x^2[1+L(c_0)^2]+4x^3[1+L(c_0)^3]+x^4[1+L(c_0)^4]\}$$

$$B_2 = 16M\{[1+Ld]+3x[1+Lc_1d]+3x^2[1+L(c_1)^2d]+x^3[1+L(c_1)^3d]\}$$

$$B_3 = 24M\{[1+L(d)^2]+2x[1+Lc_2(d)^2]+x^2[1+L(c_2)^2(d)^2]\}$$

$$B_4 = 16M\{[1+L(d)^3]+x[1+Lc_3(d)^3]\}$$

$$B_5 = 4M\{1+L(d)^4\}$$

$$B_6 = 2\{1+x\}^2$$

$$B_7 = 4\{1+x\}$$

The fraction of Hb^{3+} present in the sample is defined as:

$$f_{Hb^{3+}} = \left[\sum_{i,k=0}^{4}k(R_i^k+T_i^k)+\sum_{i,k=0}^{2}kD_i^k\right]/C_0 \qquad (17)$$

Using eqs 4–12 one has:

$$f_{Hb^{3+}}C_0 = C_1(D_0^0)^{3/2}(D_0^2)^{1/2}+C_2(D_0^0)(D_0^2)+C_3(D_0^0)^{1/2}(D_0^2)^{3/2}+C_4(D_0^2)^2+C_5(D_0^0)^{1/2}(D_0^2)^{1/2}+2(D_0^2) \qquad (18)$$

and

$$C_1 = B_2/4;\ C_2 = B_3/2;\ C_3 = 3B_4/4;\ C_4 = B_5;\ C_5 = B_7/2$$

Now we define

$$(D_0^2) = Z(D_0^0) \qquad (19)$$

and after substituting into eq. 16, one has:

$$(D_0^0)^2 f(Z,x)+(D_0^0)g(Z,x)-C_0=0 \qquad (20)$$

where

$$f(Z,x) = B_1 + B_2Z^{1/2} + B_3Z + B_4Z^{3/2} + B_5Z^2$$

$$g(Z,x) = B_6 + B_7Z^{1/2} + 2Z$$

The solution of eq. 20 is:

$$D_0^0 = \left\{ -g(Z,x) + \left[g^2(Z,x) + 4f(Z,x)C_0 \right]^{1/2} \right\} / 2f(Z,x) \quad (21)$$

By substituting into eq. 18 one has:

$$\left(D_0^0\right)^2 \left[C_1Z^{1/2} + C_2Z + C_3Z^{3/2} + C_4Z^2\right] + D_0^0\left[C_5Z^{1/2} + 2Z\right] = C_0 f_{Hb^{3+}} \quad (22)$$

Given a set of values for L, c_k, d and K_R, eq. 22 can be solved by numerical methods for each value of the oxygen pressure, to obtain the quantity Z. The quantities (D_0^0) and (D_0^2) can be calculated via eqs 19 and 21 and inserted into eq. 14 to obtain the saturation value. The final values of L, c_k, d and K_R are obtained through a best fit of eq. 14 to the entire set of experimental data, i.e., to 19 oxygen equilibrium curves measured with Hb^{3+} fractions ranging from 0 to 0.91 for a total of 304 experimental points. Fitting was performed with a non-linear least-squares algorithm that minimizes the quantity $\Gamma^2 = \sum_{i=1}^{304}[Y_i(\text{observed}) - Y_i(\text{calculated})]^2/[N-P]$, where N is the number of data points and P the number of optimizing parameters. The best-fit value of Γ^2 was 9×10^{-5}.

4.2. Mixed samples

Mixed samples were obtained by mixing aliquots of fully oxidized and fully oxygenated hemoglobin. Oxygen equilibrium measurements were made immediately after mixing to avoid further auto-oxidation of the samples. Since dimerization of tetramers occurs only via the formation of $\alpha\beta$ dimers, then only the species with zero, two or four ferric subunits are present in solution. This implies that $(D_0^1) = 0$ in eqs 8 and 10, and $R_0^2 = 2M(D_0^0)(D_0^2)$ in eq. 9, since only the tetramers in which the two ferric subunits are in the same dimer contribute to R_0^2. Thus, eqs 14, 16 and 18 become:

$$C_0Y = A_1\left(D_0^0\right)^2 + A_3'\left(D_0^0\right)\left(D_0^2\right) + A_5\left(D_0^0\right) \quad (23)$$

$$C_0 = B_1\left(D_0^0\right)^2 + B_3'\left(D_0^0\right)\left(D_0^2\right) + B_5\left(D_0^2\right)^2 + B_6\left(D_0^0\right) + 2\left(D_0^2\right) \quad (24)$$

$$f_{Hb^{3+}}C_0 = C_2'\left(D_0^0\right)\left(D_0^2\right) + C_4\left(D_0^2\right)^2 + 2\left(D_0^2\right) \quad (25)$$

The coefficients A_1, A_5, B_1, B_5, B_6, and C_4 are given in sections 4.1.2 and 4.1.3, while $A_3' = A_3/3$, $B_3' = B_3/3$ and $C_2' = C_2/3$. From the above equations one can obtain the oxygen saturation as a function of oxygen pressure, for a given set of parameters L, c_k, K_R and d.

5. Discussion

Fig. 5a shows the experimental oxygenation curves (auto-oxidized samples) and the fitting obtained using the model described above. The values of the parameters are reported in table 1 together with the standard deviations of the fits.

The data in table 1 deserve some comment:

(a) A value of the allosteric parameter L of $(1.0 \pm 0.6) \times 10^5$ is obtained from our model. This value is higher than that previously obtained under identical experimental conditions [16, 17]. This difference is due to the fact that in the previous work the presence of dimers was neglected.

(b) The value of the parameter d (0.026) is, as expected, smaller than unity but greater than the value of c_0. One also sees that the quantity Ld^4, that regulates the allosteric equilibrium of Hb^{3+}, is 4.6×10^{-2} in agreement with the fact that methemoglobin is in the R state [12]. In the presence of inositol hexaphosphate (IHP), assuming a value of $L = 10^6$–10^7 [18], one would obtain a value of $Ld^4 = 0.46$–4.6, which supports the idea that IHP converts methemoglobin to the T state [1,2].

(c) As expected, the values of the parameters c_k increase with increasing k. However, the increase is not linear. The presence of only one

Table 1

Values of the parameters obtained by fitting eq. 14 to the entire set of data points relative to oxygenation measurements for auto-oxidized samples

For the sake of completeness we also report the values of M and C_0 used in eq. 14.

L	$(1.0\pm0.6)\times10^5$
K_R	0.64 ± 0.10 mmHg
d	0.026 ± 0.003
c_0	0.0054 ± 0.0005
c_1	0.0056 ± 0.0030
c_2	0.083 ± 0.015
c_3	0.52 ± 0.14
M	4×10^5 M^{-1}
C_0	6×10^{-5} M

ferric subunit does not introduce appreciable alterations as opposed to what happens when two or three ferric subunits are present.

A check of our model was obtained with the analysis of the oxygenation curves relative to the mixed samples.

Fig. 5b shows the experimental oxygenation curves relative to these samples together with the theoretical curves. It should be stressed that the theoretical curves are drawn according to eq. 23 using the same set of parameters values listed in table 1, i.e., those obtained from fitting the measurements relative to auto-oxidized samples.

One may wonder whether the model relative to auto-oxidized samples also accounts for the oxygenation of mixed samples. Indeed, this would have been the case if redistribution of ferric subunits occurred within the time scale of our experiments. Data points resulting from a typical oxygenation experiment relative to a mixed sample are reported in fig. 6, on an expanded scale.

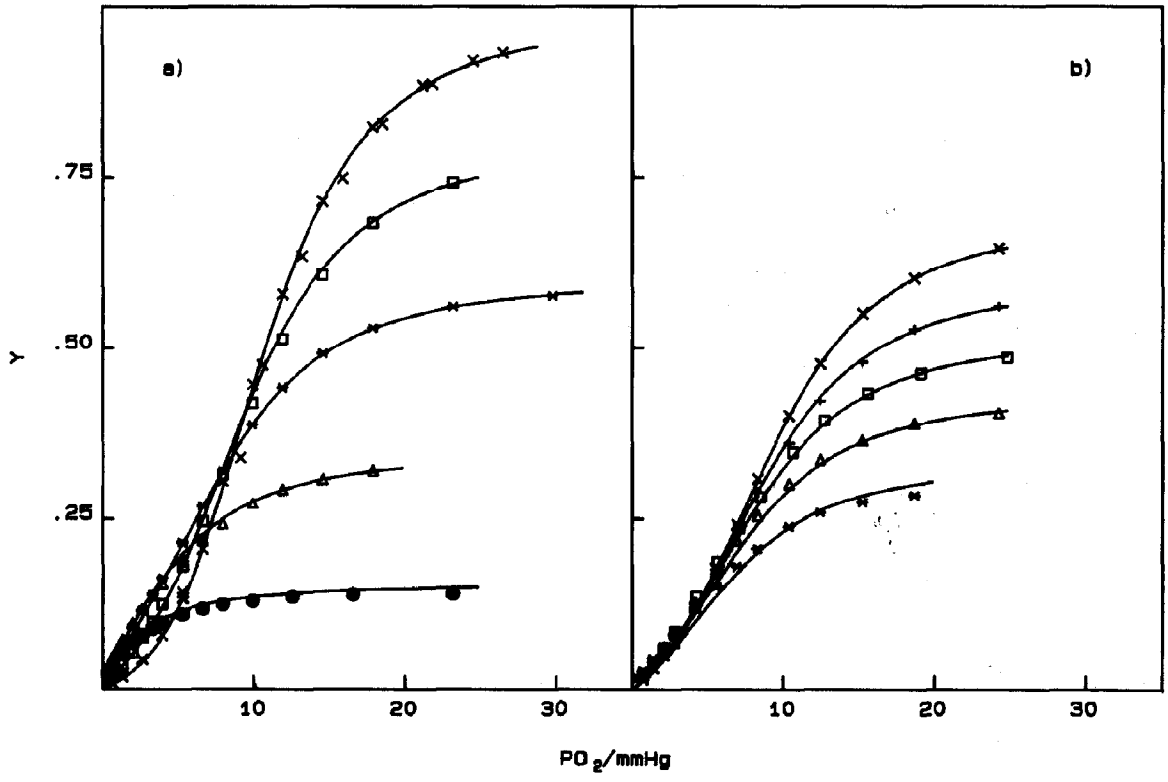

Fig. 5. (a) Oxygen saturation function relative to measurements performed in the presence of various amounts of methemoglobin (auto-oxidized samples). Symbols and percentages of oxidized hemoglobin as in fig. 2. (———) Best fits to the experimental points obtained using the model described in the text. (b) Same as in (a), for mixed samples. (×) $f_{Hb^{3+}}=0.292$, (+) $f_{Hb^{3+}}=0.383$, (□) $f_{Hb^{3+}}=0.471$, (△) $f_{Hb^{3+}}=0.558$, (*) $f_{Hb^{3+}}=0.67$. (———) Obtained using eqs 23–25 and the values of the parameters reported in table 1.

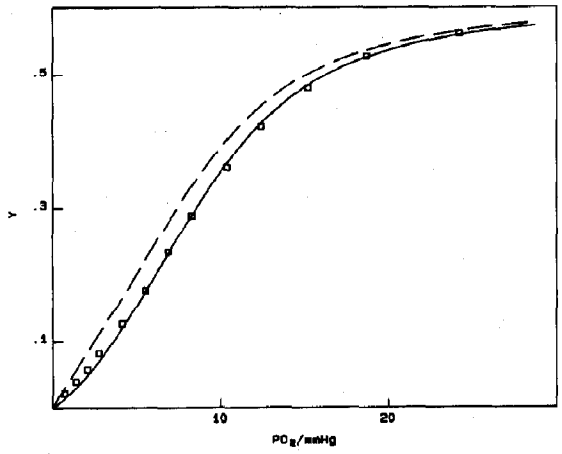

Fig. 6. Oxygen saturation function relative to a mixed sample in which $f_{Hb^{3+}} = 0.383$. (———) Theoretical curve obtained from eqs 23–25; (- - - - -) theoretical curve obtained from eqs 14, 16 and 18. For both curves the parameters values are those reported in table 1.

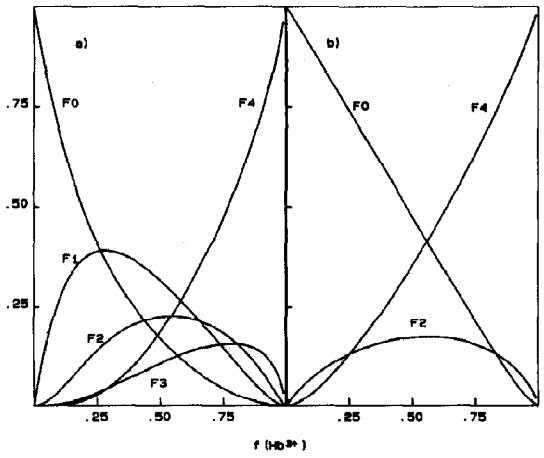

Fig. 7. Distribution of ferric subunits within fully deoxygenated tetramers as a function of the total fraction of Hb^{3+}; (a) auto-oxidized samples; (b) mixed samples. The quantities *Fk* indicate the fraction of tetramers with *k* ferric subunits.

The broken line depicts the theoretical curve obtained using eqs 14, 16 and 18, while the solid line is the curve obtained using eqs 23–25. The model modified according to the new conditions accounts for the experimental data without any need for parameter readjustment.

The distribution of ferric subunits within the tetramers in fully deoxygenated and fully oxygenated samples, as derived from our model, is shown in figs 7 and 8 as a function of the total Hb^{3+} fraction.

In the absence of oxygen, the distributions are biased toward the species F0, F1 and F4, i.e., tetramers with zero, one or four oxidized subunits, respectively. This fact explains why relatively high cooperativity levels are observed even at 50 or 60% Hb^{3+}. Moreover, the values of F0 and F4 are larger for mixed samples than for auto-oxidized samples, which implies greater values of log P_{50} and n_H. For fully oxygenated tetramers the distributions are completely different. The species with one, two or three ferric subunits are highly populated.

We believe that the different distributions obtained for fully deoxygenated and fully oxygenated samples are a consequence of the allosteric model when the dimers are taken into consideration. The longer lifetime of the T_0^0 and T_0^1 tetramers (as compared with tetramers with more ferric subunits) shifts, in the absence of oxygen, the D_0^0 and D_0^1 dimers towards the tetrameric T state. This, in turn, brings about the observed non-statistical distributions of ferric subunits within the tetramers. Conversely, since the dissociation of tetramers in the R state does not depend on the presence of

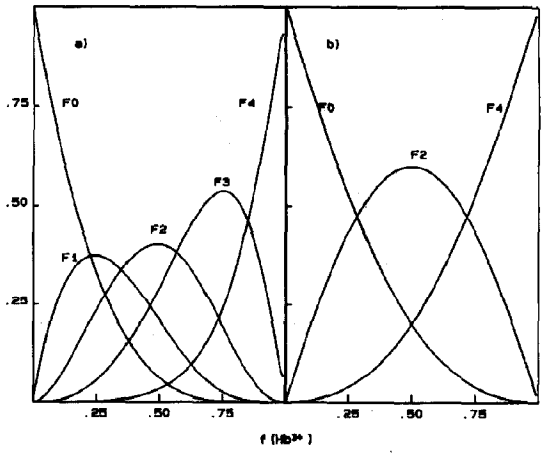

Fig. 8. Distribution of ferric subunits within fully oxygenated tetramers as a function of the total fraction of Hb^{3+}; (a) auto-oxidized and (b) mixed samples. Notation as in fig. 7.

ferric subunits, distributions closer to the statistical ones are obtained for fully oxygenated samples. The fact that F3 at 75% ferric hemes is larger than F1 at 25% can result from the fact that the presence of ferric subunits causes a slight displacement towards the T conformation that in turn stabilizes tetramers with three or four ferric subunits.

Acknowledgements

This work has been supported by MPI grants; partial indirect support has been obtained from CRRNSM.

References

1 M.F. Perutz, A.R. Fersht, S.R. Simon and G.C.K. Roberts, Biochemistry 13 (1974) 2174.
2 S. Neya and I. Morishima, J. Biol. Chem. 256 (1981) 793.
3 M.F. Perutz, G. Fermi, B. Luisi, B. Shaanan and R.C. Liddington, Acc. Chem. Res. 20 (1987) 309.
4 G. Fermi and M.F. Perutz, J. Mol. Biol. 114 (1977) 421.
5 J. Monod, J. Wyman and J.P. Changeux, J. Mol. Biol. 12 (1965) 88.
6 L. Cordone, A. Cupane, P.L. San Biagio and E. Vitrano, Biopolymers 18 (1979) 1975.
7 M.F. Perutz, Nature 237 (1972) 495.
8 J.S. Philo, M.L. Adams and T.M. Schuster, J. Biol. Chem. 256 (1981) 7917.
9 H.F. Bunn and B.G. Forget, Hemoglobin: molecular, genetic and clinical aspects (W.B. Saunders, Philadelphia, 1986).
10 A. Mansouri and K.H. Winterhalter, Biochemistry 12 (1973) 4946.
11 M.F. Perutz, Nature 228 (1970) 726.
12 R.C. Ladner, E.J. Heidner and M.F. Perutz, J. Mol. Biol. 114 (1977) 385.
13 M.A. Rosemeyer and E.R. Huehns, J. Mol. Biol. 25 (1967) 253.
14 F.C. Mills and G.K. Ackers, J. Biol. Chem. 254 (1979) 2881.
15 A.H. Chu and G.K. Ackers, J. Biol. Chem. 256 (1981) 1199.
16 L. Cordone, A. Cupane, P.L. San Biagio and E. Vitrano, Biopolymers 20 (1981) 39.
17 L. Cordone, A. Cupane and E. Vitrano, J. Mol. Biol. 189 (1986) 353.
18 K. Imai, J. Mol. Biol. 167 (1983) 741.